Since January 2020 Elsevier has created a COVID-19 resource centre with free information in English and Mandarin on the novel coronavirus COVID-19. The COVID-19 resource centre is hosted on Elsevier Connect, the company's public news and information website.

Sustainable Cities and Society 65 (2021) 102577

Contents lists available at ScienceDirect

Sustainable Cities and Society

journal homepage: www.elsevier.com/locate/scs

Living environment matters: Unravelling the spatial clustering of COVID-19 hotspots in Kolkata megacity, India

Arijit Das [a], Sasanka Ghosh [b,*], Kalikinkar Das [a], Tirthankar Basu [a], Ipsita Dutta [a], Manob Das [a]

[a] Department of Geography, University of Gour Banga, Malda, India
[b] Department of Geography, Kazi Nazrul University, Asansol, India

ARTICLE INFO

Keywords:
COVID-19
Kolkata megacity
Living environment deprivation
Containment zone
Zero-inflated negative binomial regression

ABSTRACT

The emergence of COVID-19 has brought a serious global public health threats especially for most of the cities across the world even in India more than 50 % of the total cases were reported from large ten cities. Kolkata Megacity became one of the major COVID-19 hotspot cities in India. Living environment deprivation is one of the significant risk factor of infectious diseases transmissions like COVID-19. The paper aims to examine the impact of living environment deprivation on COVID-19 hotspot in Kolkata megacity. COVID-19 hotspot maps were prepared using Getis-Ord-Gi* statistic and index of multiple deprivations (IMD) across the wards were assessed using Geographically Weighted Principal Component Analysis (GWPCA).Five count data regression models such as Poisson regression (PR), negative binomial regression (NBR), hurdle regression (HR), zero-inflated Poisson regression (ZIPR), and zero-inflated negative binomial regression (ZINBR) were used to understand the impact of living environment deprivation on COVID-19 hotspot in Kolkata megacity. The findings of the study revealed that living environment deprivation was an important determinant of spatial clustering of COVID-19 hotspots in Kolkata megacity and zero-inflated negative binomial regression (ZINBR) better explains this relationship with highest variations (adj. R2: 71.3 %) and lowest BIC and AIC as compared to the others.

1. Introduction

Coronavirus disease (COVID-19) is an epidemic illness that was discovered in Wuhan of China at the end of 2019 (World Health Organization (WHO), 2020a, 2020b). Shortly after, it spreads worldwide rapidly to emerge as a global public health concern (Das, Das, & Ghosh, 2020; Das, Das et al., 2020). As of May 3, 2020, COVID-19 has affected about 3.26 million people and claimed over 229971 deaths globally (World Health Organization (WHO), 2020c) and these figures are increasing every day. The WHO declared the COVID-19 as a global pandemic on 10th March 2020 (World Health Organization (WHO), 2020c). The United Nations (UN) realizing the wider consequences of this pandemic declared it as a social, human, and economic crisis (United Nations, 2020). UN also recognized that this pandemic will create socio-economic burdens differently in developed and developing counties of the World due to loss of human resources (United Nations, 2020).

In India, the first COVID-19 case was reported on January 30, 2020, in Kerala (Tomar & Gupta, 2020). Thereafter, big cities such as Mumbai, Ahmedabad, Pune, Chennai, and Kolkata became the epicentres of COVID-19 spreads in India (Hindustan Times, 2020a). To anticipate the COVID-19, nationwide lockdown was imposed on March 24, 2020 in India (Hindustan Times, 2020b). The COVID-19 incidences were not uniformly distributed in India and based on the risk profile of COVID-19 infection, the districts (sub-states) have been categorized into red, orange, and green zone (https://www.mohfw.gov.in).The districts with a large number of COVID-19 outbreaks and low time interval for doubling of positive cases were identified as the red zone and the districts without any COVID-19 incidence were demarcated as the green zone (https://www.mohfw.gov.in).

The districts which are not included in the red zone category and have reported at least one COVID-19 case were classified as orange zone (https://www.mohfw.gov.in). As of May 04, 2020, out of total 732 districts, 130 districts belong to the Red zones, 319 districts are in the Green zones and 284 districts are in the Orange zone across India. Kolkata megacity region belongs to the red zone, is one of the worst affected megacities in India and most affected in the state West Bengal (Kolkata megacity region reported over half of the Covid-19 cases of

* Corresponding author.
E-mail addresses: arijit3333@gmail.com (A. Das), sasankaghoshsg@gmail.com (S. Ghosh), geokinkar@gmail.com (K. Das), basu.tirthankar89@gmail.com (T. Basu), ipsitadutta25@gmail.com (I. Dutta), dasmanob631@gmail.com (M. Das).

https://doi.org/10.1016/j.scs.2020.102577
Received 15 May 2020; Received in revised form 22 October 2020; Accepted 24 October 2020
Available online 31 October 2020

West Bengal). The COVID-19 incidences reported from the neighbourhoods (residential colony and mohalla) either in the form of a large outbreak from a single location or multiple locations resulted in spatial clustering. The COVID-19 affected neighbourhoods are not uniformly distributed in Kolkata. Due to spatial clustering of COVID-19 affected neighbourhoods, cluster containment strategy has been adopted for breaking the chain of transmission to prevent its spread to other neighbourhoods. As of May 4, 2020, there are 316 such containment zones have been identified (https://wb.gov.in). These containment zones are placed under geographic quarantine for more than 40 days (on May 05, 2020, it was 41st Day lockdown) where to and from movement of population (including movement for maintaining essential services which are being provided by the local government) is not be permitted except emergency services.

Recent studies have shown multiple environmental factors such as air temperature (Liu et al., 2020; Núñez-Delgado, 2020; Wang et al., 2020; Yongjiana, Jingubc, Fengmingb, & Liqingb, 2020; Zhu & Xie, 2020), humidity (Auler et. al., 2020; Ma et. al., 2020; Gupta et. al, 2020), air pollution (Wu, Nethery, Sabath, Braun, & Dominici, 2020), smoking (Taghizadeh-Hesary & Akbari, 2020) determine the severity as well as rapid spread of COVID-19. After a quick review of the previous studies, few notable gaps have been identified. Firstly, most of the previous studies focused to examine the impact of meteorological parameters (such as air temperature, humidity, rainfall) on COVID-19 outbreak (Liu et al., 2020; Núñez-Delgado, 2020; Wang et al., 2020; Yongjiana et al., 2020; Zhu & Xie, 2020; Auler et. al., 2020; Ma et. al., 2020; Gupta et. al, 2020) rather than socio-economic conditions of the people. Secondly, Living environment deprivation, especially in megacities, may increase the risk of COVID-19 spread by affecting the survival and transmission of the virus in a variety of ways, considerable evidence exists for higher incidences of certain infectious diseases reported in an urban setting from deprived small neighbourhoods (Hughes and Gorton, 2014), overcrowded slums (Baker M, et al., 2000), and segregated low-class residential areas (Acevado-Garcia D., 2000). But still now no studies have been performed to assess the impact of overall living conditions of the households on COVID-19 cases. Thirdly, in few recent studies very few indicators have been considered to understand the urban vulnerability to COVID-19 (Misra et al., 2020; Das, Ghosh et al., 2020). However it is very difficult to understand the relationship between living conditions and COVID-19 particularly in large megacities by considering these few indicators. Fourth, very few studies have been performed to examine the relationship between living conditions of the people and outbreak of COVID-19 (Wang & Su, 2020; Wang & Wang, 2020). Particularly it remained unexplored in Indian context.

Urban living environment deprivation is a multidimensional phenomenon that results from the complex interaction of socio-demographic, socio-economic, and eco-environmental factors.The urban induced adverse eco-environmental impacts such as decreasing vegetation cover (Du et al., 2019; Gui, Wang, Yao, & Yu, 2019; Sussman, Raghavendra, & Zhou, 2019; Yao, Cao, Wang, Zhang, & Wu, 2019), increasing impervious surfaces and the concomitant rise in land surface temperature (Li, Zhang, Mirzaei, Zhang, & Zhao, 2018; Portela, Massi, Rodrigues, & Alcântara, 2020; Sejati, Buchori, & Rudiarto, 2019; Sultana & Satyanarayana, 2020; Zhang, Estoque, & Murayama, 2017; Fu & Weng, 2016; Yang, Sun, Ge, & Li, 2017; Jiang, Fu, & Weng, 2015; Fonseka et al., 2019; Bian, Ren, & Yue, 2017; Guo et al., 2015; Zhang & Sun, 2019; Arulbalaji, Padmalal, & Maya, 2020); socio-demographic factors such as the high density of population and households (HHs) negatively influences urban living environment deprivation (Niu, Chen, & Yuan, 2020; Musse et al., 2018). The urban living environment deprivation leads to deterioration of health and human comfort in cities that increases the susceptibility of infectious diseases (EPA, U., 2008). Therefore, it is logical to assess whether and how urban living environment deprivation affects the spread of COVID-19. But till now to the best of our knowledge, no study has addressed this issues on severely COVID-19 affected megacities in India. To fill-up the existing research gap, the relationship between spatial clustering of COVID-19 containment zones and living environment deprivation in Kolkata megacity has been assessed in this study. The goal of this study is to provide scientific evidence about the influence of living environment deprivation on spatial clustering of COVID-19 hotspots in Kolkata megacity. Since, the socio-economic deprivations of HHs itself are determined by multiple aspects that negatively influence the quality of living of the HH (Mishra, 2018; Baud, Pfeffer, Sridharan, & Nainan, 2009). Index of Multiple Deprivation (IMD) has been developed to examine the spatial pattern of deprivations. IMD developed by Mishra (2018) on the basis of its applicability to the context of COVID-19 using Geographically Weighted Principal Component Analysis (GWPCA) has been improved in this study. This improved variant of IMD includes non-availability of WaSH (water, sanitation, and hygiene) services within household (HH) premises which may increase the transmission rate of COVID-19 in a variety of ways (Das, Das, & Mandal, 2020). For example, the households (HH) having no availability of drinking water source and sanitation facilities within premises are more vulnerable to COVID-19 transmissions as they are dependent on community tape well or community toilets. Thus this study has an immense potentiality to understand the relationship between COVID-19 hotspots and living environment deprivation in Kolkata megacity on a robust and scientific basis.

2. Materials and methods

2.1. Study area

Kolkata megacity (22°34′N, 88°22′E) is the third-largest metropolis in India (after Mumbai and New Delhi) with a population of 4.5 million (https://censusindia.gov.in). It is the most importanturban centre in Eastern India, which has a typical subtropical, warm humid, monsoon climate classified as A_w(tropical wet and dry) in the Köppen climate classification (Kottek, Grieser, Beck, Rudolf, & Rubel, 2006). With mild and moderate winters and very hot summers, the average annual temperature and rainfall are 26.8 °C and 1582 mmrespectively (Banerjee, Chakraborty, & SenGupta, 2020). During summer months (April to June) the air temperature (T_a) often cross 40 °C with relative humidity (RH) of more than 70%. The winter (November to February) exhibits mild T_a of 25-30 °C and RH of 60%. Kolkata megacity belongs to the red zone with high COVID-19 incidences and 316 numbers of containment zones distributed heterogeneously in its 141 sub-cities (i.e. electoral wards which are the lowest administrative units). The provision of WaSH in Kolkata megacity is not satisfactory compared to other megacities of India. The scenario of WaSH is particularly poor in deprived areas reflected from low per capita availability of community latrines, stand posts, and tube well (Mukherjee et al., 2020). The lower availability of WaSH services and other factors of living environment enhances the chances of local community transmission of COVID-19 (Fig. 1).

2.2. Data Sources

To execute this study, three sources of information were used: 1) The numbers of COVID-19 containment zones were collected from the official websites of the Department of Health & Family Welfare, Govt. of West Bengal (www.wbhealth.gov.in); 2) variables required for devising IMD obtained from Census of India, 2020 (https://censusindia.gov.in); Landsat OLI/TIRS satellite images of April 6, 2020, identified by path 138 and row 44, collected from by the United States Geological Survey (USGS) 2020 website (https://earthexplorer.usgs.gov)

2.3. Methods

The steps followed in this study were outlined in Fig. 2. The processing of Landsat TM image involved enhanced band combinations, a geometric correction, conversion of digital numbers to the spectral

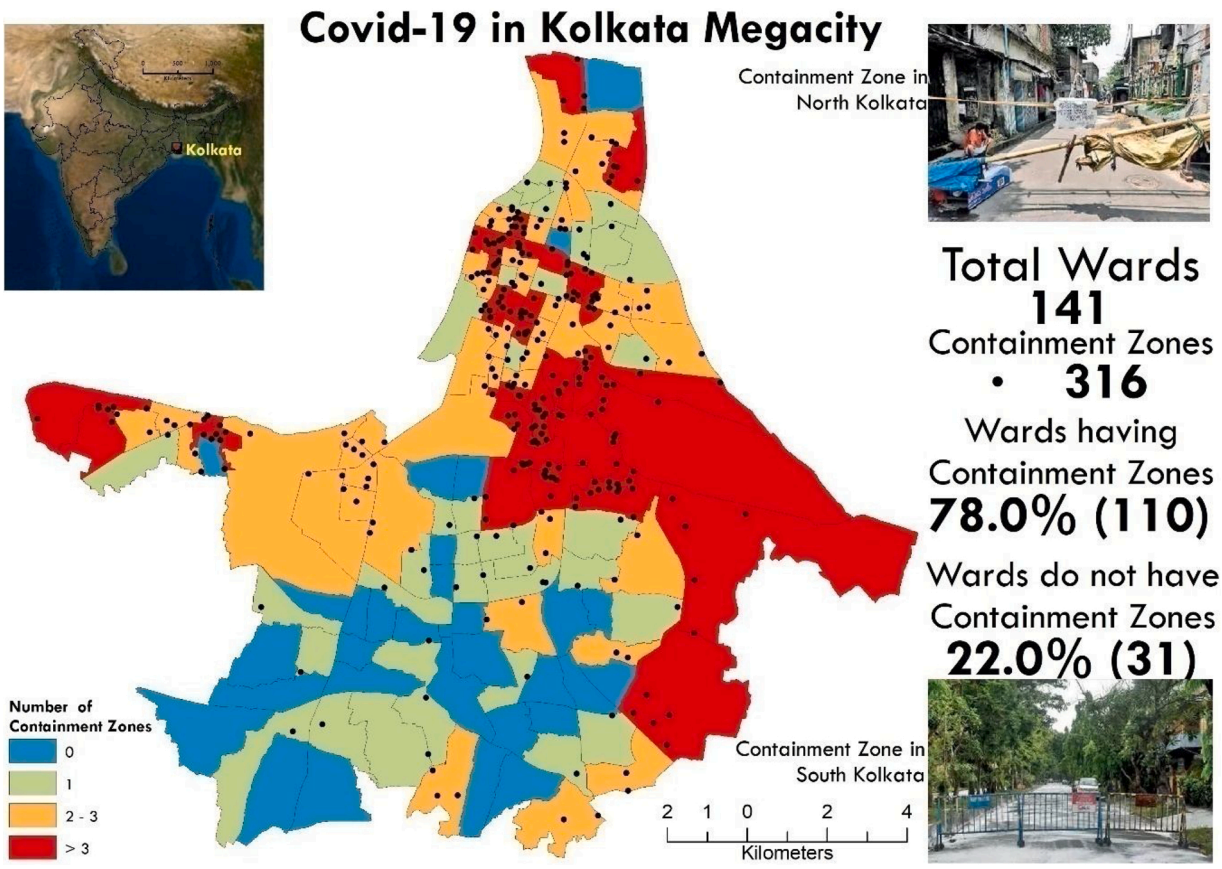

Fig. 1. The Study Area of Kolkata Megacity.

radiance of spectral bands, and finally derivation of land surface temperature (Musse, Barona, & Rodriguez, 2018). The biophysical indicators from the processed image were obtained by using the equations shown in Table 2 using the 'raster' package of the 'R' programming language.

The dimensions and indicators of urban multidimensional deprivation indices built so far varied in time and space based on objectivity. The dimensions and indicators selected to devise an IMD for 141 electoral wards of Kolkata megacity are slightly different from IMDs developed earlier (see Table 1).

2.4. Comparison of indicators considered for this study and other studies in Kolkata megacity

Before executing GWPCA to device the IMD for Kolkata megacity, the overall significance of the indicators (the factorability test) was performed by using Kaiser–Meyer–Olkin (KMO) test and Bartlett's Test of Sphericity (Antony & Visweswara Rao, 2007; Bartlett, 1950). In this study, KMO value was more than 0.800 and the chi-square value is 0.00 which indicates the indicators were very much suitable to devise IMD for Kolkata megacity. Initially, 25 indicators were selected, but 3 indictors were dropped due to multi-collinearity (1 indicator with $|r|<0.2$ dropped which was practically uncorrelated and 2 indicators dropped because they were very tightly correlated ($|r|>0.8$). The IMD is devised by employing GWPCA. GWPCA is now recognized as a very effective tool for the detection of the local non-stationary effects of variance in a data structure (Harris, Brunsdon, & Charlton, 2011; Kumar, Lal, & Lloyd, 2012; Lloyd, 2010). The local principal components and local variance derived from GWPCA are suitable in devising IMD (Mishra, 2018).

Mathematically, the local eigen decomposition of GWPCA transformation can be written in its algebraic expression as:

$$\mathrm{LVL}^{\mathrm{T}}(u, v) = \Sigma(u, v) = \mathrm{X}^{\mathrm{T}}\,\mathrm{W}(u, v)\,\mathrm{X} \tag{1}$$

W (u,v) is a diagonal matrix obtained from optimal bandwidths (here adaptive) based on the 'Bi-square' kernel weighting scheme. The details description on GWPCA is given in the Appendix A section. To reduce noise and locate important factors of IMD, the first 3 PCs with eigenvalues greater than 1 (i.e., $\lambda i \geq 1$) were retained (Hair, Black, Babin, Anderson, & Tatham, 2006).

The GWPCA derived dimension weights computed by multiplying the squared component loads and the proportion of variance explained by the corresponding PC and summing across PCs. Weights are therefore derived using Eq. 02

$$W_k = \sum_{k=1\ldots3} PC_{k,i}^2 \times \frac{\sqrt{\lambda_k}}{\sum_{j=1\ldots3}\sqrt{\lambda_j}} \tag{2}$$

W_k is the weight given to IMD Dimension *i* (either Housing Condition, Asset Possession, WaSH Services, Household Amenities and Services, and Gender disparity) $PC_{k,i}$ is the component load in k^{th} PC (column of L), k is the eigen-value of the k^{th} PC (in V) and j is the number of PCs retained (here 3).

The initial deprivation index (Si) at the sub-city level for each megacity is a weighted aggregation of components scores (C).

$$S_i = \sum_{k=1}^{m} C_i k W_k \tag{3}$$

Where, Si = Initial deprivation index, C_{ik}=Value of a component score for k^{th}PC of ward i, and W_k=Combined weight of IMD components for k^{th} PCs for Ward i, m = 3.

Applying the min-max normalization method, the initial deprivation index score for 141 wards were standardized IMD (0–100). The IMD is obtained for sub-cities of Kolkata megacity using the following formula:

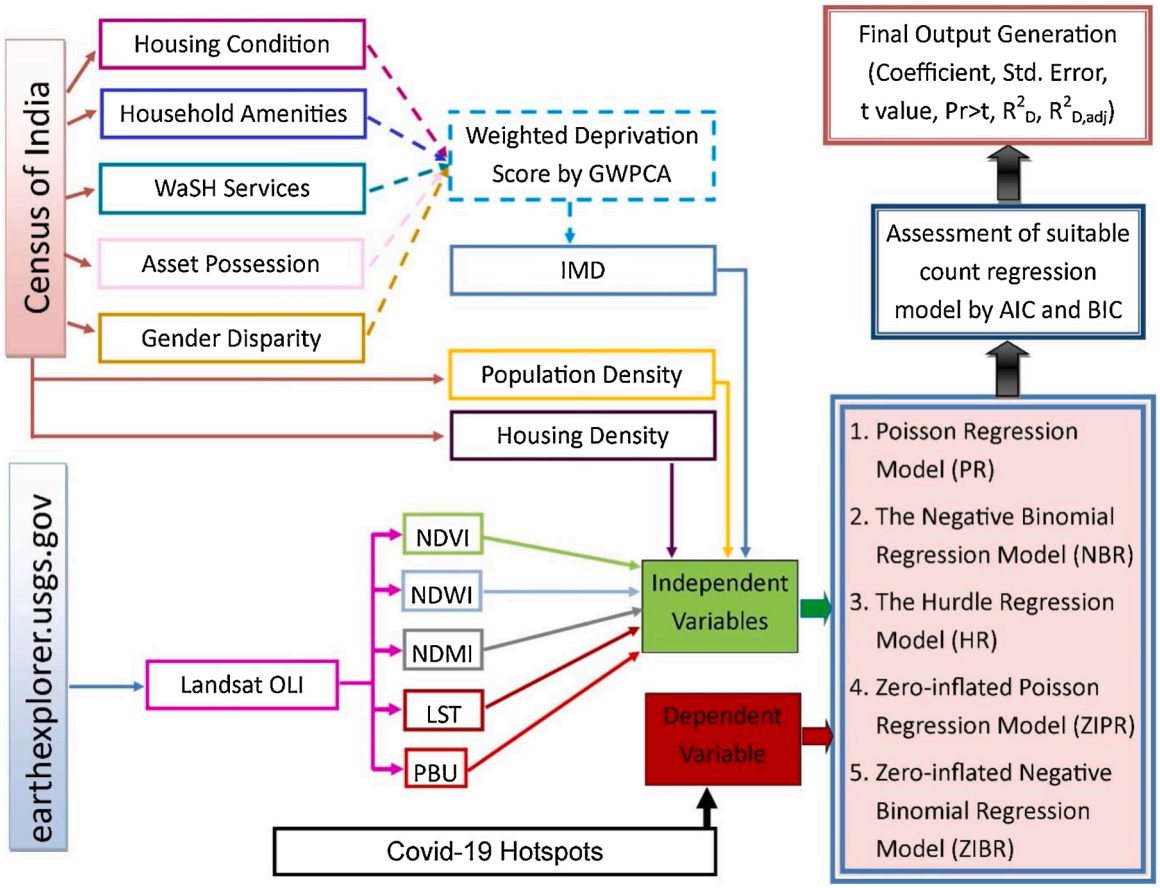

Fig. 2. Methodologicalframework of the Study.

$$IMD = \frac{S_i - S_{min}}{S_{max} - S_{min}} \times 100 \quad (4)$$

S_i, S_{min}, and S_{max} are respectively the initial deprivation score for sub-city 'i', the lowest and highest values of the initial deprivation score are considered. The construction of the final Index of Multiple Deprivation (IMD) assigns a multiple deprivation score to each urban ward for Kolkata megacity. The IMD value '0' stands for the 'bottom ranking' sub-city, 100 for the 'top-ranking' electoral ward, and varies between '0' and '100' for other wards. Essentially, it tells us where a particular sub-city stands, between the 'top' and 'bottom' ranking sub-city on a linear scale. For instance, an IMD value of 50 means that the ward is situated in the "halfway" between the top and bottom ranking wards in terms of multiple urban deprivations. The higher value of IMD correspondence to the higher level of multiple deprivations and vice versa. The IMD devised in this study was validated by comparing with the results of Baud et al. (2009) and Mishra (2018), along with information obtained from Google earth images of randomly selected 100 neighbourhoods and local knowledge.

2.5. Hotspot spatial analyses of COVID-19 containment zones and IMD

Hotspot spatial analyses are widely used in the ecological study (Chen, Chen, & Liu, 2015; Jia, Zheng, & Miao, 2018) to determine spatial clusters of high values of a particular phenomenon. In this paper, the hotspot analysis tool of ArcGIS 10.2 software (Getis-Ord Gi*) was used to explore the spatial clustering of high containment Zones of COVID-19 and high IMD values.

2.6. Statistical modelling approach

A descriptive analysis was performed for all the data. The distribution of COVID-19 containment zones was discrete and positively skewed with many wards did not have any containment zones. The distribution of COVID-19 containment zones in Kolkata megacity was negative binomial because its variance was higher than the means. 5 count data regression models (Appendix B), namely, Poisson regression (PR), negative binomial regression (NBR), hurdle regression (HR), zero-inflated Poisson regression (ZIPR), and zero-inflated negative binomial regression (ZINBR) are considered to analyse the impact of living environment deprivation on the spatial distribution of COVID-19 containment zones in Kolkata megacity. The explanatory factors considered to perform the regression analysis are listed in Table 2. The best count data regression model is obtained by comparing the values of the likelihood ratio (LR) test, Akaike's information criterion (AIC), the Bayesian information criterion (BIC), and the adjusted coefficient of determination (R^2adj). The values of AIC, BIC, and R^2adj are acquired using the following formula (Pinheiro & Bates, 2000; Zeng, 2015).

$$AIC = -2\log Lik + 2(p+1)$$
$$BIC = -2\log Lik + (p+1)\log(n) \quad (5)$$

$$R^2adj = 1 - \frac{(n-1)\sum_{i=1}^{n}\left(yi - \widehat{yi}\right)^2}{(n-p)\sum_{i=1}^{n}(yi - \overline{yi})^2} \quad (6)$$

Where, yi, $\widehat{yi}$, $\overline{yi}$ sequentially are observed value, the estimated value, and the mean value of the biomass; n is the number of samples; p is the number of parameters; $t_a$is the t value at confidence level with n–p degree of freedom; and logLik is the log-likelihood values of the non-linear regression model. The two-sided statistical analyses were carried out at a

Table 1
Domains and variables of Index of Multiple Deprivation of Kolkata megacity.

Domains	Variable Category	Variables	S V Mishra (2018)	ISA baud (2008)	Other(s)
Housing Condition	Type of structure of Census house	% of HH does not have a concrete roof			Das & Mistri, 2013
	Ownership	% of HH lives in a house not owned by them	*		Mishra, 2018
	Permanent House	% of HH having a semi-permanent or temporary structure			Das & Mistri, 2013
	HH with the single dwelling room	% of HH with the single dwelling room			Das & Mistri, 2013
Asset Possession	Banking	% of HH do not have access to banking facility	*	*	Isa Baud etal. (2008)
	Radio	% of HH not owned radio			Das & Mistri, 2013
	Television	% of HH not owned television			Das & Mistri, 2013
	Computer and Laptop	% of HH do not have a computer or laptop			Das & Mistri, 2013, Bhan & Jana, 2015
	Telephone and Mobile Phone	% of HH without telephone or mobile phone			Das & Mistri, 2013, Bhan & Jana, 2015
	Bicycle	% of HH do not own bicycle			Das & Mistri, 2013
	Scooter/Motorcycle/ moped	% of HH do not own scooter or Motorcycle or moped		*	Isa Baud et al. (2008)
	Car/Jeep/Van	% of HH do not owna car or jeep or van			Das & Mistri, 2013
	None of the Specified Assets	% of HH not having any of the assets- radio/ transistor, television, computer/ laptop (with or without internet), telephone/ mobile phone, scooter/ motorcycle/moped, car/jeep/van	*		Mishra, 2018
WaSH Services	Location of Drinking water	% of HH with the location of water source not within their premises			Das & Mistri, 2013
	Latrine Facility	% of HH with no latrine facility within the premise	*	*	Baud et al. (2008), McGranahan, 2015, Mishra, 2018
	Waste Water Disposal	% of HH with wastewater outlet is connected to Open and no drainage	*		Mishra, 2018
	Source of Drinking water	% of HH obtain drinking water from untreated sources	*		Mishra, 2018
Household Amenities and Services	Cooking fuel	of HH using non-clean fuel for cooking			Das & Mistri, 2013
	Kitchen	% of HH Have no separate kitchen			Das & Mistri, 2013
	Source of Lightning	% of HH with a source of lightning in the house is environmentally polluting	*	*	Baud et al. (2008)
Gender Disparity	Literacy	female illiteracy rate			Das & Mistri, 2013
	Worker	% of female Non-worker			Das & Mistri, 2013

Table 2
COVID-19 containment zones and its determining factors.

Indicators	Equation
Dependent Variable	
Ward wise Number of Containment Zones	NA
Explanatory Factors	
Urban Patch Density (UPD)	Number of urban Patch/ Hectare Area
Land Surface Temperature (LST)	$TB = \frac{K_2}{\ln\left(\frac{K_1}{L_\lambda}+1\right)} \times \ln\varepsilon$
Normalized Differential Vegetation Index (NDVI)	$NDVI = \frac{(NIR - RED)}{(NIR + RED)}$
Normalized Differential Water Index (NDWI)	$NDWI = \frac{(NIR - SWIR)}{(NIR + SWIR)}$
Normalized Differential Moisture Index (NDMI)	$NDMI = \frac{(SWIR1 - NIR)}{(SWIR1 + NIR)}$
Index of Multiple Deprivation (IMD)	
Population Density (PPD)	Population/ Area
Household Density (HHD)	No. of Household/ Area

5% level of significance. All analyses were conducted using R software (version 3.5.3) with the "glm" and "pscl" package.

In some previous research studies, deprivation of the households were assessed across cities using GWPCA (Basu & Das, 2020; Charlton, Brunsdon, Demsar, Harris, & Fotheringham, 2010). But recent studies reported that there were a close association of COVID-19 transmissions and living condition of the households (Wang & Su, 2020; Wang & Wang, 2020). For example, urban slums are more vulnerable to infectious diseases due to lack of availability, accessibility of households to the basic services and amenities (Arifeen et al., 2001; Checkley et al., 2016; Corburn et al., 2020). Thus it is clear that living environment of the households largely influence transmissions of infectious diseases. In this study, an attempt has been made to examine the impact of living environment on COVID-19 transmissions using Index of Multiple Deprivation (IMD) for the first time in India. Most of the recent studies tried to interlink COVID-19 transmissions with WASH (water, sanitation and hygiene) provisions but ignored overall living conditions of the households. In addition to this, the COVID-19 hotspot maps were prepared (i) to understand the high-high and low-low concentrations of COVID-19 and (ii) to examine the relationship between COVID-19 hotspots and deprivation within the city. Thus the findings of this method will surely assist to overall living environment of the households.

The regression models (Poisson regression (PR), negative binomial regression (NBR), hurdle regression (HR), zero-inflated Poisson regression (ZIPR), and zero-inflated negative binomial regression (ZINBR)) were also used to assess the impact of living environment on COVID-19 hotspot in Kolkata megacity.

3. Results

3.1. Spatial distribution of deprived areas in Kolkata megacity

To analyze the distribution of deprived areas, this study categorizes IMD into five different classes of multiple deprivations based on equal interval methods, with IMD $\leq$ 20.00 as least deprived and IMD $>$ 80.00 as a most deprived category. Table 3, is showing the distribution of wards across five IMD categories. The wards with IMD values $>$ 60 were considered as deprived and 16.94 percent of the total wards belong to

Table 3
Distribution of deprived wards.

Deprivation Criteria	IMD	
	No. of Wards	Percentage of Population
0 to 20.0 (Least Deprived)	17	9.57
20.1 to 40.0	47	32.18
40.1 to 60.0	59	41.30
60.1 to 80.0	15	14.20
80.1 to 100 (Most Deprived)	03	2.74

this category.

As per the result of the study, it was observed that maximum number of wards (59) fall under the deprivation criteria between 40.1 and 60.0 (41.39 % population) followed by the criterion of 20.1–40.0 (47 wards comprising 32.18 % of population), 0–20.0 (17 wards comprising 9.58 % of population), 60.1–80.0 (15 wards comprising 14.20 % of population) respectively.

3.2. Geography of multiple deprivations of Kolkata megacity

The spatial extent and distribution of IMD are unable to explore the geography of multiple deprivations in Kolkata megacity. The spatial heterogeneity of multiple deprivations in Kolkata megacity was examined using spatial hotspot analyses using the following formula:

$$G_i^* = \frac{\sum_{j=1}^{n} w_{i,j}x_j - \overline{X}\sum_{j=1}^{n} w_{i,j}}{S\sqrt{\frac{\left[n\sum_{j=1}^{n} w_{i,j}^2 - \left(\sum_{j=1}^{n} w_{i,j}\right)^2\right]}{n-1}}} \quad (7)$$

Where xj is the feature attribute value for j, $w_{i,j}$ represents spatial weight value between feature i and j, n indicating total number of features.

Whereas $\overline{X} = \sum_{j=1}^{n} x_j$ and $S = \sqrt{\frac{\sum_{j=1}^{n} x_j^2}{n} - \left(\overline{X}\right)^2}$

Hotspots of COVID-19 containment and multiple deprivations identified by IMD had obvious overlapping areas. Approximately 60.6 % of the COVID-19 hotspot area and 51.6 % of the multidimensional area deprivation was located in northern and central parts of the city (Fig. 3). Most of the COVID-19 hotspots were reported from northern and central parts of the city that makes these areas COVID-19 hotspot within the city. Interestingly large proportions of areas (>50 %) with multidimensional deprivation were concentrated in particularly northern part of the city. In northern part of the city most of the urban slums are located. In addition to this, large proportion of multidimensional deprivation in northern part within the city clearly suggests that there are lacks of availability, accessibility as well as inequalities of basic services and amenities to the people in the city (see supplementary section) (Table 4).

3.3. Relationship between COVID-19 hotspots and living environment deprivation

The result of the study showed that COVID-19 hotspots are mainly concentrated in areas with relatively less availability as well as accessibility of basic services and amenities. Therefore it is necessary to find out the relationship of COVID-19 hotspot with living environmental parameters. As per as spearman's correlation coefficients, COVID 19 containment has significantly negative relationship with LST ($r = -0.633$, $p = 0.008$) NDVI ($r = -0.75$, $p = 0.004$), NDWI ($r = -0.413$, $p = 0.048$), and positive correlation with IMD ($r = 0.823$, $p = 0.001$), PPD ($r = 0.734$, $p = 0.006$), HHD ($r = 0.532$, $p = 0.007$); UPD ($r = 0.431$, $p = 0.043$) and no statistically significant relationship with NDMI ($r = 0.391$). The interrelation of IMD with various eco-environmental indicators was also very striking. However, the socio-economic variables are negatively correlated with eco-environmental variables (Fig. 4).

For a better presentation of the relationship between COVID-19 containment clustering (hotspots) and its various covariates of living environment deprivation, we have selected four clusters (2 from COVID-19 hotspots and 2 from Cold Spot) namely Window-A, Window-B, Window-C, and Window-D. Table 5 shows the cluster-specific distribution of COVID-19 containment zones and their association with living environment characteristics. It is clear from Table 5 that there are striking differences in the living environment deprivation between COVID-19 hotspots and cold spots. This provides strong initial evidence that the living environment deprivation has a strong influence on spatial clustering of hotspots in Kolkata megacity.

3.4. Zero-inflated negative binomial regression analysis

The descriptive analysis was performed for all the data. Table 6 summarizes the descriptive statistics for IMD, remotely sensed metrological, and other socio-demographic variables. The mean of IMD, PPD, HHD, UPD, LST, NDVI, NDWI, and NDMI were 41.69 (with Max. = 100, Min. = 0.00, S.D = 17.25), 40,738 persons/km^2 (with

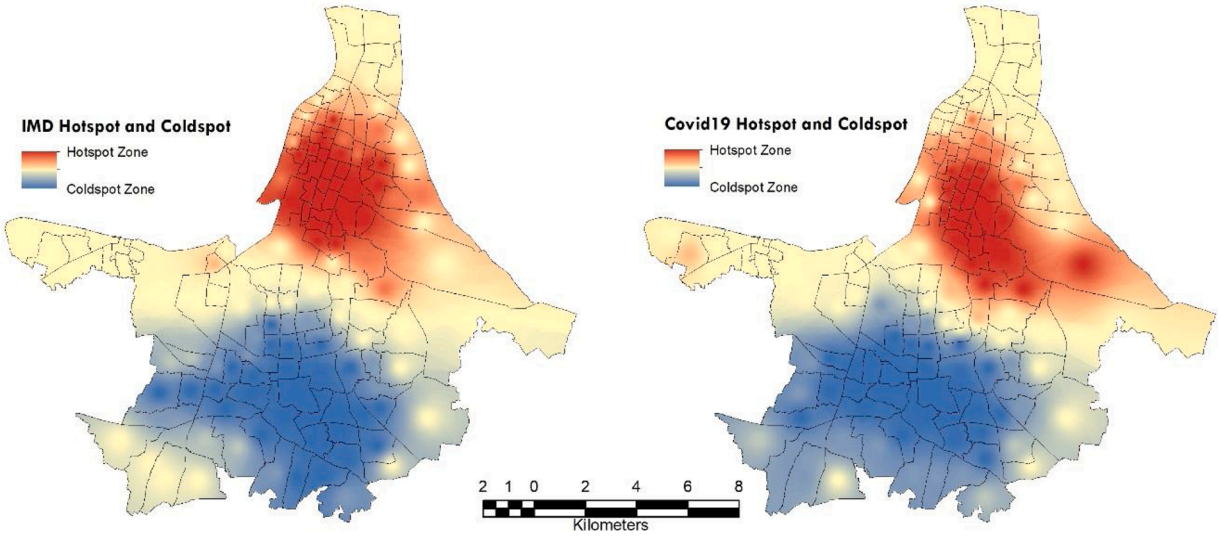

Fig. 3. Spatial Clustering of Containment Zones of COVID-19 and IMD values.

Table 4
Spearman's correlation coefficients between indicators.

	Frequency of Containment Zones	IMD	PPD	HHD	UPD	LST	NDVI	NDWI	NDMI
Frequency of Containment Zones	1	0.823**	0.734**	0.532**	0.431*	−0.633**	−0.675**	−0.413*	0.391
IMD	0.823**	1	0.434*	0.228	0.390*	0.376*	−0.370*	0.093	0.115
PPD	0.734**	0.434*	1	0.972**	0.618**	0.745**	−0.780**	0.752**	−0.766**
HHD	0.532**	0.228	0.972**	1	0.662**	0.729**	−0.791**	0.763**	−0.800**
UPD	0.431*	0.390*	0.618**	.662**	1	0.703**	−0.817**	0.771**	−0.877**
LST	−0.633**	0.376*	0.745**	0.729**	0.703**	1	−0.827**	−0.811**	−0.791**
NDVI	−0.675**	−0.370*	−0.780**	−0.791**	−0.817**	−0.827**	1	0.994**	0.923**
NDWI	−0.413*	0.093	0.752**	0.763**	0.771**	−0.811**	0.994**	1	-.885**
NDMI	0.391	0.115	−0.766**	−0.800**	−0.877**	−0.791**	0.923**	−0.885**	1

** Correlation is significant at the 0.01 level (2-tailed).
* Correlation is significant at the 0.05 level (2-tailed).

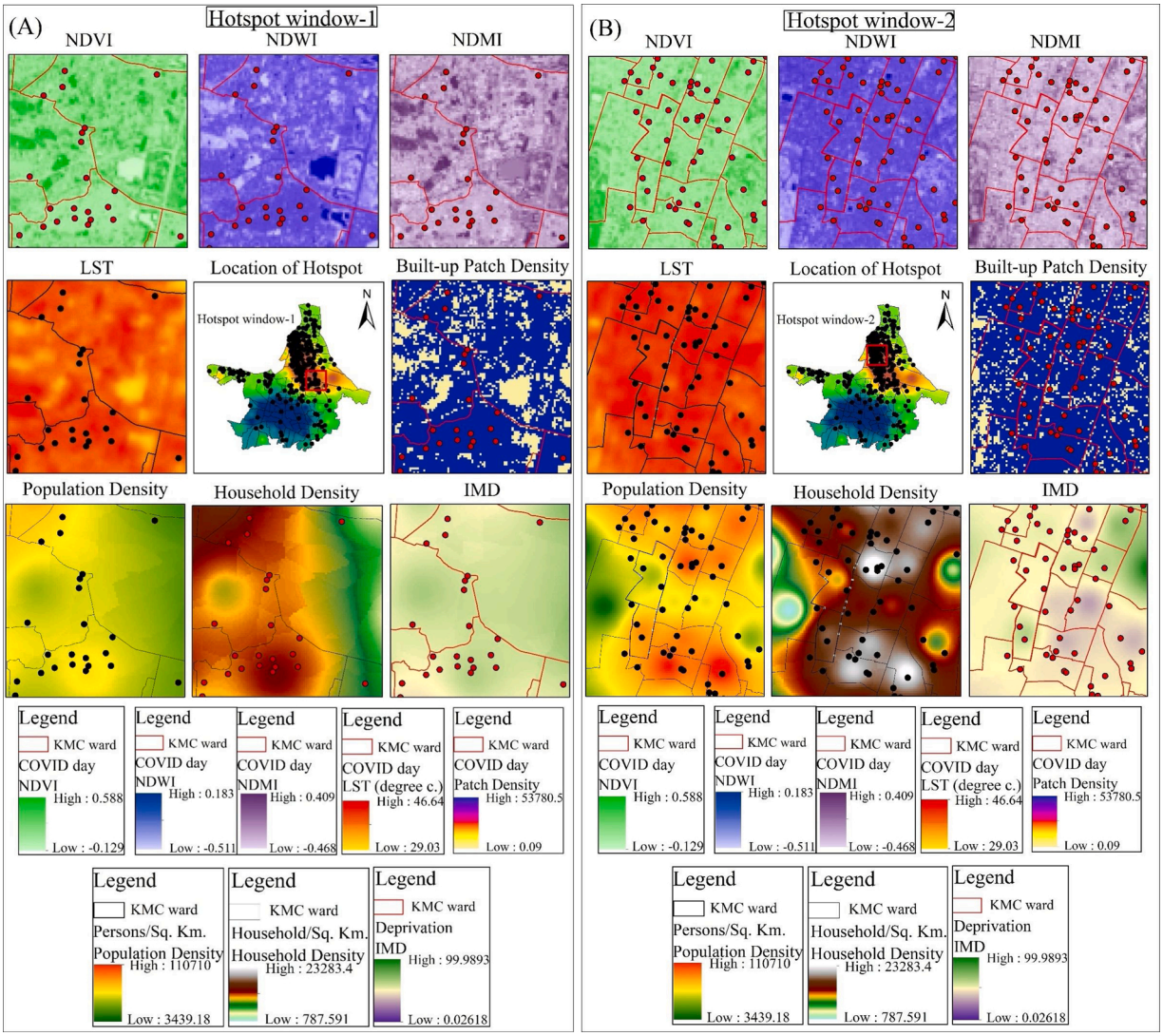

Fig. 4. Clustering patterns of COVID-19 containment zones and its relationship with socio-economic, socio-demographic and bio-physical covariates.

Max. = 111067.00, Min. = 3427.33, S.D = 25378.56), 8805.00 HH/km^2 (with Max. = 23295.00, Min. = 785.00, S.D = 4709.00), 42917.59/hect. (with Max. = 52768.16, Min. = 17467.14, S.D = 7018.02), 38.77 °C (with Max. = 41.83, Min. = 33.65, S.D = 1.68), 0.16 (with Max. = 0.27, Min. = 0.07, S.D = 0.04), -0.14 (with Max.= -0.24, Min.= -0.07, S.D = 0.03), and 0.03 (with Max. = 0.14, Min.= -0.03, S.D = 0.03), respectively.

The comparisons of test statistics presented in Table 7 and the values of LR, AIC, and BIC indicate that the ZINBR model was the best fit for this study. The value of LR, AIC, and BIC is lowest for the ZINBR, which suggests that the model is better. ZINBR with two-sided tests, and $p < 0.05$ was considered statistically significant.

Estimated coefficients from the ZIPR and ZINBR models are presented in Table 8 for comparison purposes. Although both the ZIPR and ZIBR model identify IMD, PPD, and LST as significant contributors to the COVID-19 containment zones, HD, PPD, and NDMI were added as

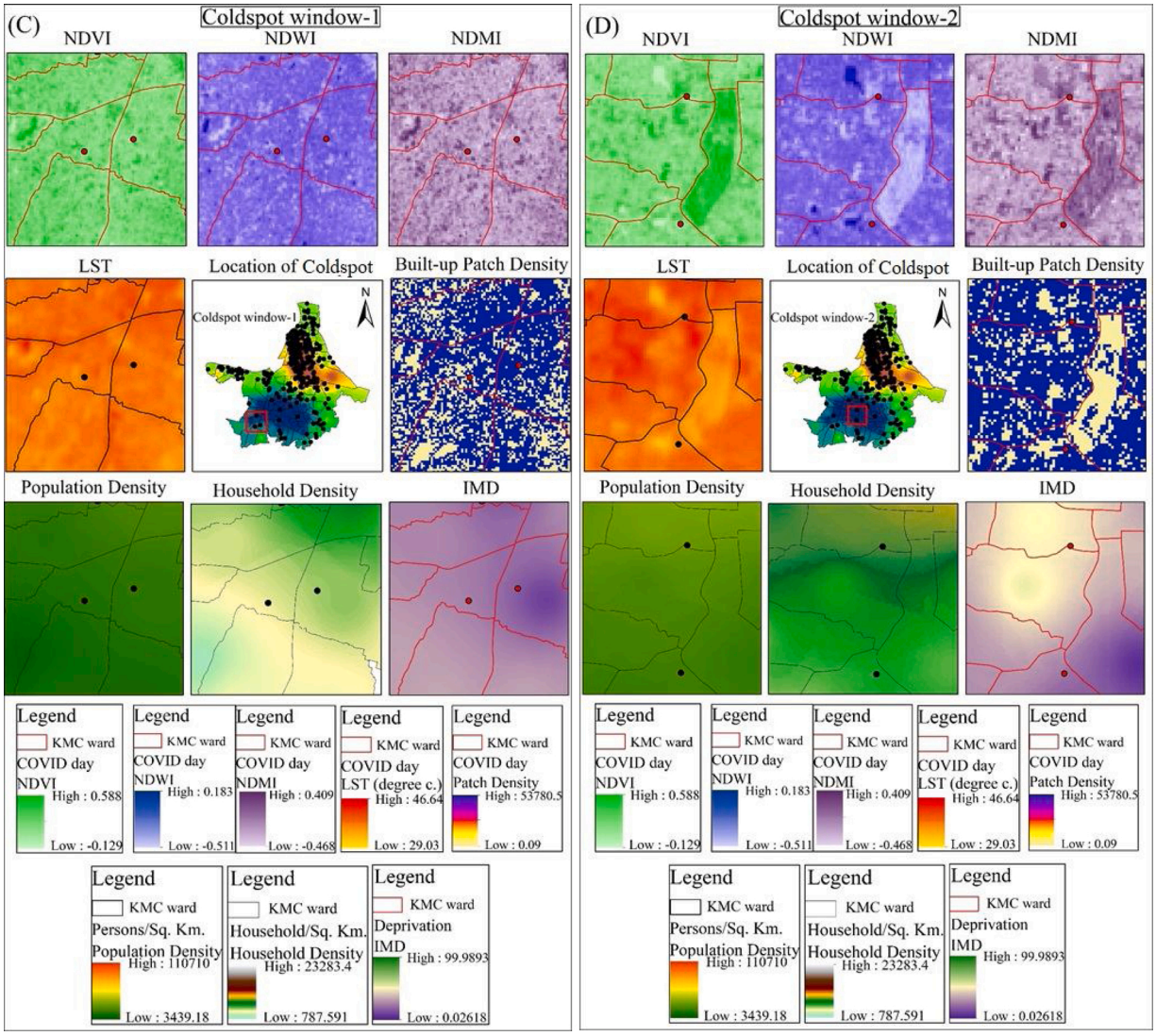

Fig. 4. (*continued*).

Table 5
Cluster specific condition of living environment and Distribution of COVID-19.

Window	Constituents Ward/Part	No. of containment zone	LST	NDVI	NDWI	NDMI	UPD	HHD	PD	IMD
A	58,57,56,59,65,66,108	22	36.41	0.03	0.17	−0.15	35,091	7980	37,662	44.32
B	63,62,54,55,53,52,46,47,50,51,36,48,49,45,44,40,37,43	52	37.53	0.01	0.13	−0.11	46187	11570	57013	43.43
C	121,122,123,125,124, 125, 126, 127	2	48.13	0.07	0.22	−0.20	31038	4384	16928	37.14
D	89,117,118,94,98,116,97,115,121,122	2	40.43	0.05	0.19	−0.17	33951	6221	24039	31.72

additional significant predictors by the better fitting ZINBR count data model.

When all other variables were constant, according to ZIPR the wards with high IMD probability of having COVID-19 containment zones was 37 % higher compared to the wards with lower IMD ($RR = e^{0.321} = 1.38$, 95 % CI 1.14–1.62). Whereas, as per the estimate of ZINBR, the wards with high IMD, chances of having COVID-19 containment zones was 121 % higher compared to the wards with lower IMD ($RR = e^{0.754} = 2.21$, 95 % CI 1.97–2.45). Similarly, wards with high HHD have 88 % higher chances of having COVID-19 containment zones compared to the wards with lower housing density ($RR = e^{0.632} = 1.88$, 95 % CI of 1.64–2.12). Also, the wards with higher LST have 35 % ($RR = e^{-0.425} = 0.65$, 95 % CI of 0.41 to 0.89) lower chances of having COVID-19 containment zones compared to the wards with lower LST (Table 9).

4. Discussion

In this research, we compiled 35 variables that could potentially explain the spatial pattern of COVID-19 hotspots in Kolkata megacity. These variables were grouped into two different aspects that determine the living environment deprivation, namely socio-economic and eco-environmental. A synthetic IMD was developed by employing GWPCA and using local variance as the weight for the dimensions. The widely used PCA cannot account for the local variance (Harris et al., 2011; Kumar et al., 2012; Lloyd, 2010). In this paper, hotspot analysis employed to explore the spatial clustering of COVID-19 containment Zones. Finally, an ensemble of IMD and other remotely sensed eco-environmental variables used to model (ZIBR) the geographic distribution of COVID-19 containment zones in Kolkata megacity. It was

Table 6
Descriptive Statistics for different variables.

Pearson's Product-Moment Correlation	N	Maximum (Max.)	Minimum (Min.)	Mean	Std. Deviation (S.D)
Number of Covid-19 Containment Zones	141	14	0	2.24	9.22
IMD		100.00	0.00	41.69	17.25
PPD		111067.00	3427.33	40738.78	25378.56
HHD		23295.00	785.00	8805.00	4709.00
UPD		52768.16	17467.14	42917.59	7018.02
LST		41.83	33.65	38.77	1.68
NDVI		0.27	0.07	0.16	0.04
NDWI		−0.24	−0.07	−0.14	0.03
NDMI		0.14	−0.03	0.03	0.03

Table 7
Test statistics comparison of Models Model.

Variable	Model*				
Test statistic	PR	NBR	HR	ZIPR	**ZIBR**
Log likelihood (*-2ℓ*)	−6011	−3196	−4065	−3116	**-3026**
Akaike's information criterion (AIC)	12224	9221	8139	7889	**6890**
Bayesian information criterion (BIC)	12454	9312	8435	8216	**7356**
R^2_D	54.1	56.3	50.1	52.3	**72.2**
$R^2_{D,adj}$	53.6	54.3	49.7	51.2	**71.3**

found that the spatial context of COVID-19 containment zones was better explained by ZIBR compared to the other count regression models. ZIBR provided more reliability and flexibility in studying the spatial extent of COVID-19 containment in response to living environment deprivation. Based on our findings, a combination of four variables IMD, PPD, HD, and LST could explain the high variability (i.e. heterogeneous distribution) of the COVID-19 containment zones in Kolkata megacity. Continued monitoring of the areas in Kolkata megacity with relatively higher levels of living environment deprivation factors can improve the understanding of COVID-19 spreads in Kolkata megacity.

At the time of writing this manuscript, the Kolkata megacity was worst affected in the state of West Bengal with 316 number of containment zones spatially clustered in the northern and the central zone of the megacity have observed a large outbreak of COVID-19. The findings of ZIBR suggested a strong positive relationship of COVID-19 outbreaks and living environment deprivation in Kolkata megacity. This further strengthens the findings Ahmed, Ahmed, Pissarides, and Stiglitz (2020)) that the socioeconomic disadvantages and inequalities have a profound role in the spread of COVID-19. As the COVID-19 continues to spread, the areas with low social status of households and unfavourable demographic condition have more susceptibility to be affected like what happens in the United States (Mollalo, Mao, Rashidi, & Glass, 2019). Apart from these previous literatures, in recent studies it was well recognized that various types of infectious diseases like COVID-19 are largely determined by the living conditions of the people (Ahmed et al., 2020; Bhutta, Sommerfeld, Lassi, Salam, & Das, 2014; Patel et al., 2020). The living conditions of the people affect COVID-19 transmissions in a variety of way. Firstly, generally the economically weaker people reside in overcrowded areas (high population density).

Table 8
Estimated coefficients for ZIPR and ZIBR in predicting the number of containment zones of COVID-19 in Kolkata megacity.

Variable	Models							
	ZIPR				ZINBR			
Explanatory Variables	Coef.	Std.error	t value	Pr > t	coef.	Std.error	t value	Pr > t
Constant (*y*)	1.124	0.044	10.16	<0.001	2.157	0.039	12.16	<0.001
IMD	0.321	0.012	7.26	<0.001	0.754	0.010	8.28	<0.001
PPD	0.280	0.030	4.16	0.030	0.531	0.293	6.36	<0.003
HHD	0.285	0.070	4.56	0.091	0.632	0.015	5.86	<0.002
UPD	0.004	0.415	1.26	0.060	0.041	0.315	4.26	0.072
LST	−0.344	0.423	−5.52	<0.001	0.425	−0.425	−6.42	<0.004
NDVI	−0.212	0.120	−2.36	0.112	−0.003	−0.154	−2.35	0.092
MDWI	0.008	0.008	1.24	0.295	0.002	0.019	1.64	0.082
NDMI	0.004	0.009	1.36	0.306	0.251	0.121	1.52	0.042

Table 9
Summary of the previous studies on living environment deprivation.

Author(s)	Study area	Socio Economic Indicator	Eco-Environmental Indicators	Total Indicators
I.S.A. Baud et al. (2009)	Chennai, Delhi and Mumbai(India)	10	0	10
S.V. Mishra (2018)	Kolkata(India)	5	4	9
Lo (1997)	Georgia (USA)	4	3	7
Li and Weng (2007)	Indianapolis (USA)	8	2	10
Nichol and Wong (2009)	Hong Kong (China)	2	3	5
Escobar Jaramillo (2010)	Cali (California)	5	7	12
Santana, Escobar Jaramillo, and Capote (2010)	Cali (California)	0	5	5
Liang and Weng (2011)	Indianapolis (USA)	13	6	19
Ogneva-Himmelberger, Rakshit, and Pearsall (2012)	Massachusetts (USA)	9	7	16
Rao, Kant, Gahlaut, and Roy (2012)	Uttarakhand (India)	4	3	7
De Deus, Garcia Fonseca, Marcelhas, and De e Souza (2013)	Uberlandia (Brazil)	7	7	14
Rahman, Kumar, Fazal, and Bhaskaran (2011)	New Delhi (India)	4	4	8
Stathopoulou, Iacovides, and Cartalis (2012)	Athens (Greece)	5	3	8
Joseph, Wang, and Wang (2014)	Port-au-Prince (Haiti)	5	7	12
Stossel, Kissinger, and Meir (2015)	Haifa, Tel Aviv and Beer Sheva (Israel)	1	19	20
Silva and Mendes (2012)	Viana do Castelo (Portuguese)	0	7	7

Thus overcrowded or high population density is an important factor of infectious disease transmissions (Ai, Zhang, & Zhang, 2016; Alaniz, Bacigalupo, & Cattan, 2017; Jia et al., 2020) even in case of COVID-19 transmissions (Sun et al., 2020, Kodera, Rashed, & Hirata, 2020; Rocklöv & Sjödin, 2020). Secondly, access to basic services and amenities (housing conditions, water availability, sanitations, limited outdoor spaces) can also affect respiratory disease as well as deadly COVID-19 transmissions (Das, Das et al., 2020; Mishra et al., 2020; Naddeo & Liu, 2020). Thirdly, the areas with socio-economically deprived are highly vulnerable because the people living in these areas are often employed in such an occupations that are not provide opportunities to work at their home. Thus from the overall analysis it was clear that the living conditions (or living environment) are closely linked with the transmissions of COVID-19. In this study also it was well documented that northern part of Kolkata megacity are relatively high vulnerable due to high population density as well as relatively limited availability as well as accessibility to the basic services and amenities of the people. The result also clearly suggests that there was an impact of living environment on COVID-19 transmissions. The findings suggested that socio-economic dynamics must be incorporated for formulating mitigation strategies to combat COVID-19 pandemic situation.

In most of the recent studies, the factors affecting COVID-19 transmissions were assessed either from different perspectives considering population density (Kodera et al., 2020; Rocklöv & Sjödin, 2020; Sun et al., 2020), meteorological parameters such as temperature, humidity, wind speed, pressure, rainfall (Xie and Zhu, 2020; Yongjian et al., 2020; Liu et al., 2020; Wang et al., 2020; Auler, Cássaro, & da Silva, 2020; Ma et al., 2020; Gupta, Ghosh, Singh, & Misra, 2020; Wu et al., 2020; Jiang and Xu., 2020). However, to the best of our knowledge, no studies were performed previously to examine the impact of living environment (living conditions) in relation to COVID-19 transmissions.

A deprived household can be defined as the lack of accessibility as well as availability to the basic services and amenities. Thus limited access to the basic services and amenities influence overall living conditions of the households (Das, Das et al., 2020; Saroj, Goli, Rana, & Choudhary, 2020). Particularly the people living in slum like conditions are relatively more vulnerable to infectious disease due to limited access to basic services and amenities (Corburn et al., 2020; Mishra et al., 2020). More than 30 % of the total urban population in Kolkata lives in slum areas. Most of the slums are located in eastern and western (dock area) and northern (Cossipore) part of the city. Ray (2016), performed a study over some selected slums in Kolkata and findings of the study showed that there were only one community tap for entire slum areas (about 600 people collect water from this community tape). As per as findings of Bag and Seth (2016), more than 70 % slum dwellers are dependent on public sanitation facilities in Delhi, Kolkata and Mumbai. Being COVID-19 an infectious disease, is it not vulnerable for entire slum population? If there is single COVID-19 positive slum dweller, will it not increase the risk of COVID-19 transmissions? In previous studies it was also well documented that deprive people had very limited access to the basic services and amenities (Goswami, 2014; Phukan, 2014; Sajjad, 2014). Recent studies also reported that provision of basic services had significant impact on COVID-19 transmissions (Das, Das et al., 2020; Corburn et al., 2020; Mishra et al., 2020). Thus from the overall analysis, it was clear that deprivations of households may have significant impact on the formations of COVID-19 hotspots in Kolkata megacity also.

In Northern part of Kolkata, the population density is relatively high as compared to south Kolkata. In recent studies it was well recognized that the transmissions of COVID-19 is largely determined by population density (Carozzi, 2020; Kodera et al., 2020; Rashed, Kodera, Gomez-Tames, & Hirata, 2020; Rocklöv & Sjödin, 2020). Thus from overall analysis, it was clear that there were a strong positive correlation between population density and COVID-19 transmissions. Thus in North Kolkata, high population density may have a significant factor for COVID-19 transmission as compared to other parts of the megacity.

In developing countries, environmental issues received very less attentions in policy making framework and most of the time environmental degradation moves parallel with economic development (Das & Das, 2019b). Environmental factors (such as vegetation cover, land surface temperature, water bodies etc.) are largely influenced by socio-demographic and economic factors (such as population density, living environment of the households, household density). In recent studies it was documented that socio-demographic factors have crucial impact on COVID-19 (Sannigrahi, Pilla, Basu, Basu, & Molter, 2020; Kumar et al., 2020). In this study also, it was recorded that socio-economic status (living environment of the households) has an impact on COVID-19 transmissions. In developing countries like India, unplanned and haphazard expansion of cities not only affect quality of urban people but also degradation of environment (such as loss of forest cover, water etc.) (Capps, Bentsen, & Ramírez, 2016; Shahbaz, Sbia, Hamdi, & Ozturk, 2014; Azam & Khan, 2016; Das & Das, 2019a; 2019b; Chun, Wei, & Xin, 2020). In Kolkata megacity also, rapid urban expansion causes deteriorations of ecosystem health (Ghosh, Chatterjee, & Dinda, 2019; Das, Das et al., 2020). Thus from the previous studies, it was well recognized that there were a strong nexus between socio-economic and environmental factors.

Based on our study, three remotely sensed eco-environmental factors (LST, NDVI, and PDU) have influential role spatial clustering of COVID-19 incidence in Kolkata megacity. The findings are similar to previous studies (Ma et al., 2020), but unlike these studies which have used meteorological data, we have obtained the eco-environmental data using remote sensing for the first time to explore the impact of bio-physical indices on COVID-19 incidences. While we did not find NDWI and MNDWI to be significantly influential in COVID-19 incidences.

4.1. Implementation of policies

A number of responses were created by the government across the world to reduce the rapid transmissions of COVID-19 such as lockdown, closing of shopping malls, travel restrictions, restrictions of public gatherings, investment in health care facilities etc. In spite of these policies, the cities across the globe were severely affected by this deadly disease (Misra et la., 2020). More than 90% of the total cases were reported from urban areas and 1400 cities of world are severely affected (UN-Habitat, 2020). In India also it was well recognized that the large cities are severely affected such as Mumbai, Delhi, Chennai, Hydrabad, Jaipur, Jodhpur, Ahamedabad etc. More than 50% of the total COVID-19 confirmed cases were reported from ten large cities in India. As per as recent report of Indian Council of Medical Research (ICMR), risk of COVID-19 transmissions was 1.09 time higher in urban areas and 1.89 times higher in urban slum areas respectively (Swarajya, 2020). Thus from the above findings, it was obvious that the urban areas are more vulnerable to COVID-19 transmissions. The findings also clearly showed that only above mentioned policies are not enough to reduce the COVID-19 transmissions rather government must focus on the living environment of the urban dwellers and priority must be given on the availability as well as accessibility to the basic services and amenities (such as water, sanitations, housing conditions etc).

Government must provide adequate basic services and amenities to the poor urban dwellers to improve the quality of life through existing programmes such as Jawaharlal Nehru Urban Renewal Mission (JNNURM), Integrated Housing and Slum Development Programs (IHSDP). The local government must focus on the proper effectiveness of policies and programmes without politicize. In addition to this, urban planners and policy makers must need deep research before implementation of any urban planning framework in future.

5. Conclusion

The study analyses the impact of living environment on COVID-19 hotspots in Kolkata megacity. The study also used a number of

statistical tools to understand the impact of living environment on COVID-19 hotspot in the city. As per as findings of the study, it was well recognized that the clusters of COVID-19 hotspots are largely determined by the availability as well as accessibility to the basic services and amenities (that determine the level of living conditions of the households). The result of the study documented that the concentrations of COVID-19 hotspots were relatively high in northern part of the city. Interestingly in northern part of the city population density was high with higher concentrations urban slums population. Such outcome of the study clearly suggests that there was strong association of COVID-19 hotspot areas with living conditions of the study. Thus this study has great scientific contributions towards the urban policy making framework to combat with infectious disease in future. A number of multiple indicatorsthat influences living environment deprivation have been grouped into socio-economic and eco-environmental for better understanding the impact on spatial distribution of COVID-19 containment zones in Kolkata megacity. A synthetic IMD using advanced local static-GWPCA has been developed to examine the spatial pattern of deprivation within the city. Five regression models have been used and the performance of best fitted model (ZIBR) has been compared with other four count regression models. As per statistical modelling approaches, it was well recognized that the areas with high risk of COVID-19 incidences spill-over to occur in upcoming days. The findings of the study revealed the similar result performed by Mollalo et al. (2019) as it was recorded that living environment deprivation has a profound impact on the spatial distribution of COVID-19 containment zones in Kolkata megacity. To the best of our knowledge, still now there are limited studies over large as well as severely COVID-19 affected megacities across the world. Thus, this study can be regarded as a basis for future modelling of COVID-19 incidences at the megacity level as well as to understand the relationship between living environment of the households and COVID-19 hotspots.

One of the limitations of this study was the availability of the finest spatial granularity COVID-19 positive cases at the electoral ward level. However, the identification, containment areas and adaptation of strict geographic quarantine measures in these containment zones indicate the large outbreaks of COVID-19 in these areas. Therefore, making inferences on COVID-19 based on the spatial distribution of COVID-19 is not problematic until or unless an appropriate and best fit statistical analysis (count regression models in general and ZIBR in particular) is used to model the association between COVID-19 hotspots and living environment deprivation.

Declaration of Competing Interest

The authors report no declarations of interest.

Appendix A

Geographically Weighted Principal Component Analysis (GWPCA)

GWPCA analysis helps to access the local level statistics, which utilizes the geographically weighted variance-covariance matrix to acquire the geographically weighted mean (Eq. A01) (Lloyd, 2010):

$$\overline{y}_{ij} = \frac{\sum_{j=1}^{n} y_i w_{ij}}{\sum_{j=1}^{n} w_{ij}} \tag{A1}$$

Following this, the geographical weights can be obtained by employing the Gaussian weighting scheme (Eq. A02) (Forheringham et al., 2002):

$$w_{ij} = \exp[-0.5(d_{ij}/\tau)^2] \tag{A2}$$

Here, d_{ij} = inter-distance between the locations i and j. τ = bandwidth that signifies the kernel size.

Later on, by standardizing the geographic weights to one, then, geographic mean will be as:

$$\overline{y} = \sum_{j=1}^{n} y_j w_{ij} \tag{A3}$$

Geographically weighted standard deviation is acquired using Eq. A04 (Lloyd, 2010).

$$\sqrt{\sigma_i} = \left[\sum_{j=1}^{n} (y_j - y_i)^2 w_{ij}\right]^{1/2} \tag{A4}$$

Geographically weighted covariance of variables y_1 and y_2 for location i is obtained by (Eq.A05) (Lloyd, 2010):

$$\mathrm{cov}(y_{1i}, y_{2i}) = \sum_{j=1}^{n} w_{ij}(y_{1j} - \overline{y}_{1i})(y_{2j} - \overline{y}_{2i}) \tag{A5}$$

Finally, geographically weighted correlation coefficient is computed by Eq. A06(Lloyd, 2010):

$$r_i = \frac{\mathrm{cov}(y_{1i}, y_{2i})}{\sqrt{\sigma(y_{1i})\sigma(y_{2i})}} \tag{A6}$$

Where $\sigma(y_{1i})$ and $\sigma(y_{2i})$ = Geographically weighted variances at location 'i' for the variables 'y_1' and 'y_2'. The obtained correlation matrix is used to derive the PC for each location.

Appendix B. % count regression model

In the following regression models, the number of COVID-19 affected contaminated zones is selected as dependent variables and the independents variables are deprivation score of Kolkata, population density, housing density, Normalized Difference Vegetation Index (NDVI), Normalized Difference Water Index (NDWI), Normalized Difference Moisture Index (NDMI), Land Surface Temperature (LST), and Patch Built-up (PBU).

The Poisson Regression Model

In this regression, it is assumed that the Poisson incidence rate (μ) can be determined by the set of 'k' regressor variables (the X's). This relation can be expressed as Eq. A07. (https://ncss-wpengine.netdna-ssl.com/wp-content/themes/ncss/pdf/Procedures/NCSS/Poisson_Regression.pdf)

$$\mu = t\exp(\beta_1 X_1 + \beta_2 X_2 + ... + \beta_k X_k) \tag{A7}$$

Where $X_1 \equiv 1$; β_1 = intercept; The regression coefficient β_1,β_2, ….. β_k represents the unknown parameters which are estimated from a data set. Following this notation, The Poisson regression model can be expressed for the observation 'i' as equation 12

$$\Pr(Y_i = y_i|\mu_i, t_i) = \frac{e^{-\mu_i t_i}(\mu_i t_i)^{y_i}}{y_i!} \tag{A8}$$

Where

$$\mu_i = t_i \mu(x'_i \beta)$$

$$= t_i \exp(\beta_1 X_{2i} + ... + \beta_k X_{ki})$$

Here Y = Dependent variables; X = Independent or regressor variables; t = Exposure values

The Negative Binomial Regression Model

In this regression model, a set of 'k' regressor variable and the exposure time 't' are used to determine the mean of 'y'. The following relation can be expressed as Eq. A09 (https://ncss-wpengine.netdna-ssl.com/wp-content/themes/ncss/pdf/Procedures/NCSS/Negative_Binomial_Regression.pdf)

$$\mu = \exp(ln(t_i) + \beta_1 x_{1i} + \beta_2 x_{2i} + ... + \beta_k x_{ki}) \tag{A9}$$

Where $X_1 \equiv 1$; β_1 = intercept; The regression coefficient β_1,β_2, ….. β_k represents the unknown parameters which are estimated from a data set and the estimates are epitomized as b_1, b_2, …., b_k.Following this notation, the negative binomial regression model can be expressed for the observation 'i' as Eq. A10

$$\Pr(Y_i = y_i|\mu_i, \alpha) = \frac{\Gamma(y_i + \alpha^{-1})}{\Gamma(\alpha^{-1})\Gamma(y_i + 1)}\left(\frac{1}{1+\alpha\mu_i}\right)^{a^{-1}}\left(\frac{\alpha\mu_i}{1+\alpha\mu_i}\right)^{y_i} \tag{A10}$$

Here Y = Dependent variables; X = Independent or regressor variables; t = Exposure values; α = Dispersion parameter which is estimated from the data by employing maximum likelihood.

The Hurdle Regression Models

The hurdle model can be written as Eq. A11 (Hofstetter, Dusseldorp, Zeileis, & Schuller, 2016)

$$P(Y_i = y_i|x_i, z_i, \beta, \gamma) = \begin{cases} f_{zero}(0; z_i; \gamma), \\ (1 - f_{zero}(0; z_i; \gamma))\dfrac{f_{count}(y_i; x_i; \beta)}{1 - f_{count}(0; x_i; \beta)} \end{cases} \tag{A11}$$

Where y_i = dependent variable value for the i th observation 'i' = 1, …, N), z_i = vector of length 'J' denoting the predictor variables number in the zero part, χ_i = vector of length 'K' denoting predictor variables numbers in the hurdle part, γ = vector of coefficients which belongs to 'z', and β = vector of coefficients which is related to 'x' [Zeileis, Kleiber, & Jackman, 2008]. f_{zero} = probability density function at least on {0, 1} (binary) or {0, 1, 2, …} (count), and f_{count} = probability density function on {0, 1, 2, …}.

The Zero-inflated Poisson Regression Model

The zero-inflated poisson model deals with the two zero generating processes. The first one deals with the generation of the zero and the second one is associated with the Poisson distribution which generates counts. Within these counts, some of may be zero. The following fixates can be described as Eq. A12

$$\Pr(y_j = 0) = \pi + (1 - \pi)e^{-\lambda}$$

$$\Pr(y_j = h_i) = (1 - \pi)\frac{\lambda^{h_i}e^{-\lambda}}{h_i!}, h_i \geq 1 \tag{A12}$$

Where y_j = the outcome variable with the value of any non-negative integer; λ = expected poisson count at the 'i' th observation; π represents the probability of the extra zeros.

References

Ahmed, F., Ahmed, N. E., Pissarides, C., & Stiglitz, J. (2020). Why inequality could spread COVID-19. *The Lancet Public Health, 5*(5), e240.

Alaniz, A. J., Bacigalupo, A., & Cattan, P. E. (2017). Zika: Probability of establishment of its vector, Aedes aegypti, in Chile. *Revista chilena de infectologia: organo oficial de la Sociedad Chilena de Infectologia, 34*(6), 553–556.

Antony, G. M., & Visweswara Rao, K. (2007). A composite index to explain variations in poverty, health, nutritional status and standard of living: Use of multivariate statistical methods. *Public Health, 121*(8), 578–587. https://doi.org/10.1016/j.puhe.2006.10.018

Arifeen, S., Black, R. E., Antelman, G., Baqui, A., Caulfield, L., & Becker, S. (2001). Exclusive breastfeeding reduces acute respiratory infection and diarrhea deaths among infants in Dhaka slums. *Pediatrics, 108*(4), e67.

Arulbalaji, P., Padmalal, D., & Maya, K. (2020). Impact of urbanization and land surface temperature changes in a coastal town in Kerala, India. *Environmental Earth Sciences, 79*(17), 1–18.

Auler, A. C., Cássaro, F. A. M., da Silva, V. O., et al. (2020). Evidence that high temperatures and intermediate relative humidity might favor the spread of COVID-19 in tropical climate: A case study for the most affected Brazilian cities. *Science of the Total Environment*. https://doi.org/10.1016/j.scitotenv.2020.139090

Azam, M., & Khan, A. Q. (2016). Urbanization and environmental degradation: Evidence from four SAARC countries—Bangladesh, India, Pakistan, and Sri Lanka. *Environmental Progress & Sustainable Energy, 35*(3), 823–832.

Bag, S., & Seth, S. (2016). Understanding standard of living and correlates in slums: An analysis using monetary versus multidimensional approaches in three Indian cities. *Delhi School of Economics, Centre for Development Economics Working Paper, 263*, 17-01.

Banerjee, I., Chakraborty, S., & SenGupta, S. (2020). Silhouette of M87*: A new window to peek into the world of hidden dimensions. *Physical Review D, 101*(4), Article 041301.

Bartlett, M. S. (1950). Tests of significance in factor analysis. *British Journal of Statistical Psychology, 3*(2), 77–85. https://doi.org/10.1111/j.2044-8317.1950.tb00285.x

Basu, T., & Das, A. (2020). Formulation of deprivation index for identification of regional pattern of deprivation in rural India. *Socio-Economic Planning Sciences*, Article 100924.

Baud, I. S. A., Pfeffer, K., Sridharan, N., & Nainan, N. (2009). Matching deprivation mapping to urban governance in three Indian mega-cities. *Habitat International, 33*(4), 365–377. https://doi.org/10.1016/j.habitatint.2008.10.024

Bhan, G., & Jana, A. (2015). Reading spatial inequality in urban India. *Economic and Political Weekly, 50*(22), 49.

Bhutta, Z. A., Sommerfeld, J., Lassi, Z. S., Salam, R. A., & Das, J. K. (2014). Global burden, distribution, and interventions for infectious diseases of poverty. *Infectious Diseases of Poverty, 3*(1), 21.

Bian, T., Ren, G., & Yue, Y. (2017). Effect of urbanization on land-surface temperature at an urban climate station in North China. *Boundary-Layer Meteorology, 165*(3), 553–567.

Capps, K. A., Bentsen, C. N., & Ramírez, A. (2016). Poverty, urbanization, and environmental degradation: urban streams in the developing world. *Freshwater Science, 35*(1), 429–435.

Carozzi, F. (2020). *Urban density and COVID-19*.

Census of India (https://censusindia.gov.in).

Charlton, M., Brunsdon, C., Demsar, U., Harris, P., & Fotheringham, S. (2010). *Principal components analysis: From global to local*.

Checkley, W., Pollard, S. L., Siddharthan, T., Babu, G. R., Thakur, M., Miele, C. H., … Van Schayck, O. C. (2016). Managing threats to respiratory health in urban slums. *The Lancet Respiratory Medicine, 4*(11), 852–854.

Chen, Y.ue, Chen, M.eichao, Liu, B.eiyuan, et al. (2015). The methodology function of CiteSpacemapping knowledge domains. *Journal Science Studies, 33*(2), 242–253.

Chun, Y., Wei, Z., & Xin, Y. (2020). Coupling coordination evaluation and sustainable development pattern of geo-ecological environment and urbanization in Chongqing municipality, China. *Sustainable Cities and Society*, 102271. https://doi.org/10.1016/j.scs.2020.102271

Corburn, J., Vlahov, D., Mberu, B., Riley, L., Caiaffa, W. T., Rashid, S. F., … Jayasinghe, S. (2020). Slum health: arresting COVID-19 and improving well-being in urban informal settlements. *Journal of Urban Health*, 1–10.

Das, M., & Das, A. (2019a). Dynamics of Urbanization and its impact on Urban Ecosystem Services (UESs): A study of a medium size town of West Bengal, Eastern India. *Journal of Urban Management, 8*(3), 420–434. https://doi.org/10.1016/j.jum.2019.03.002

Das, M., & Das, A. (2019b). Estimation of Ecosystem Services (EESs) loss due to transformation of Local Climatic Zones (LCZs) in Sriniketan-Santiniketan Planning Area (SSPA) West Bengal, India. *Sustainable Cities and Society, 47*, Article 101474. https://doi.org/10.1016/j.scs.2019.101474

Das, M., Das, A., & Mandal, A. (2020). *Ecosystem Health (EH) Assessment of a rapidly urbanizing metropolitan city region of Eastern India- A study on Kolkata Metropolitan Area.* https://doi.org/10.1016/j.landurbplan.2020.103938

Das, A., Das, M., & Ghosh, S. (2020). Impact of nutritional status and anemia on COVID-19: Is it a public health concern? Evidence from National Family Health Survey-4 (2015–2016), India. *Public Health, 185*, 93.

Das, A., Ghosh, S., Das, K., Dutta, I., Basu, T., & Das, M. (2020). (In) visible impact of inadequate WaSH Provision on COVID-19 incidences can be not be ignored in large and megacities of India. *Public Health*, 10.1016%2Fj.puhe.2020.05.035.

De Deus, L. R., Garcia Fonseca, L. M., Marcelhas, & De e Souza, I. (2013). *Creating an socioenvironmental condition index to assess of urban environmental quality. Urban Remote Sensing Event (JURSE)* (pp. 271–274). Sao Paulo: IEEE. https://doi.org/10.1109/JURSE#.2013.6550717

Du, J., Fu, Q., Fang, S., Wu, J., He, P., & Quan, Z. (2019). Effects of rapid urbanization on vegetation cover in the metropolises of China over the last four decades. *Ecological Indicators, 107*, Article 105458.

EPA, U. (2008). *Registration eligibility science chapter for chlorpyrifos: fate and environmental assessment* (2002). Environmental Protection Agency.

Escobar Jaramillo, L. A. (2010). *El valor económico de la calidad ambiental urbana.* p. 306. Cali, Colombia: Universidad del Valle.

Fonseka, H. P. U., Zhang, H., Sun, Y., Su, H., Lin, H., & Lin, Y. (2019). Urbanization and its impacts on land surface temperature in Colombo metropolitan area, Sri Lanka, from 1988 to 2016. *Remote Sensing, 11*(8), 957.

Fu, P., & Weng, Q. (2016). A time series analysis of urbanization induced land use and land cover change and its impact on land surface temperature with Landsat imagery. *Remote Sensing of Environment, 175*, 205–214.

Ghosh, S., Chatterjee, N. D., & Dinda, S. (2019). Relation between urban biophysical composition and dynamics of land surface temperature in the Kolkata metropolitan area: a GIS and statistical based analysis for sustainable planning. *Modeling Earth Systems and Environment, 5*(1), 307–329.

Goswami, S. (2014). The hidden transcripts of the slums. *Global Journal of Human-Social Science, 14*(3), 63–73.

Gui, X., Wang, L., Yao, R., & Yu, D. (2019). Investigating the urbanization process and its impact on vegetation change and urban heat island in Wuhan, China. *Environmental Science and Pollution Research, 26*(30), 30808–30825.

Guo, G., Wu, Z., Xiao, R., Chen, Y., Liu, X., & Zhang, X. (2015). Impacts of urban biophysical composition on land surface temperature in urban heat island clusters. *Landscape and Urban Planning, 135*, 1–10.

Gupta, R., Ghosh, A., Singh, A. K., & Misra, A. (2020). Clinical considerations for patients with diabetes in times of COVID-19 epidemic. *Diabetes & Metabolic Syndrome, 14*(3), 211–212. https://doi.org/10.1016/j.dsx.2020.03.002. Advance online publication.

Hair, J. F., Black, W. C., Babin, B. J., Anderson, R. E., & Tatham, R. L. (2006). *Multivariate data analysis*. Uppersaddle River. NJ: Pearson Prentice Hall.

Harris, P., Brunsdon, C., & Charlton, M. (2011). Geographically weighted principal components analysis. *International Journal of Geographical Information Science, 25*(10), 1717–1736. https://doi.org/10.1080/13658816.2011.554838

Hindustan Times. (2020a). *PM Modi announces all-India lockdown over Covid-19, will be in place for 21 days*. Retrieved May 03, 2020, from. https://www.hindustantimes.com/india-news/pm-modi-to-address-nation-on-coronavirus-shortly/story aR7ugx57A8sRiXX5MHAcpL.html. (March 24, 2020).

Hindustan Times. (2020b). *Top 10 worst-hit cities account for over 50% of total Covid-19 cases in India.* Retrieved May 06, 2020, from. https://www.hindustantimes.com/india-news/covid-19-update-top-10-worst-hit-cities-account-for-over-50-of-total-covid-19-cases-in-india/story-aFSH3ddWfClXcFttm5SsYN.html(May 05, 2020).

Hofstetter, H., Dusseldorp, E., Zeileis, A., & Schuller, A. A. (2016). Modeling Caries Experience: Advantages of the Use of the Hurdle Model. *Caries Research, 50*, 517–526. https://doi.org/10.1159/000448197

Jia, L., Zheng, X., & Miao, J. (2018). Research progress and hotspot analysis of spatial interpolation. *IOP Conference Series: Earth and Environmental Science, 113*, 012079. https://doi.org/10.1088/1755-1315/113/1/012079

Jiang, Y., Fu, P., & Weng, Q. (2015). Assessing the impacts of urbanization-associated land use/cover change on land surface temperature and surface moisture: A case study in the midwestern United States. *Remote Sensing, 7*(4), 4880–4898.

Joseph, M., Wang, F., & Wang, L. (2014). GIS-based assessment of urban environmental quality in Port-au-Prince, Haiti. *Habitat International, 41*, 33–40. https://doi.org/10.1016/j.habitatint.2013.06.009

Kodera, S., Rashed, E. A., & Hirata, A. (2020). Correlation between COVID-19 morbidity and mortality rates in Japan and local population density, temperature, and absolute humidity. *International Journal of Environmental Research and Public Health, 17*(15), 5477.

Kottek, M., Grieser, J., Beck, C., Rudolf, B., & Rubel, F. (2006). World map of the Köppen-Geiger climate classification updated. *Meteorologische Zeitschrift, 15*(3), 259–263.

Kumar, S., Lal, R., & Lloyd, C. D. (2012). Assessing spatial variability in soil characteristics with geographically weighted principal components analysis. *Computational Geosciences, 16*(3), 827–835.

Li, G., & Weng, Q. (2007). Measuring the quality of life in city of Indianapolis by integration of remote sensing and census data. *International Journal of Remote Sensing, 28*(2), 249–267. https://doi.org/10.1080/01431160600735624

Li, G., Zhang, X., Mirzaei, P. A., Zhang, J., & Zhao, Z. (2018). Urban heat island effect of a typical valley city in China: responds to the global warming and rapid urbanization. *Sustainable Cities and Society, 38*, 736–745. https://doi.org/10.1016/j.scs.2018.01.033

Liang, B., & Weng, Q. (2011). Assessing Urban environmental quality change of Indianapolis, United States, by the remote sensing and GIS integration. *IEEE Journal of Selected Topics in Applied Earth Observations and Remote Sensing, 4*(1), 43–55. https://doi.org/10.1109/JSTARS.2010.2060316

Liu, J., Zhou, J., Yao, J., Zhang, X., Li, L., Xu, X., He, X., Wang, B., Fu, S., Niu, T., Yan, J., Shi, Y., Ren, X., Niu, J., Zhu, W., Li, S., Luo, B., & Zhang, K. (2020). Impact ofmeteorological factors on the COVID-19 transmission: amulti-city study in China. *Science Total Environment*. https://doi.org/10.1016/j.scitotenv.2020.138513. Elsevier.

Lloyd, C. D. (2010). Analysing population characteristics using geographically weighted principal components analysis: A case study of northern Ireland in 2001. *Computers, Environment and Urban Systems, 34*(5), 389–399. https://doi.org/10.1016/j.compenvurbsys.2010.02.005.

Lo, C. P. (1997). Application of Landsat TM data for quality of life assessment in an urban environment. *Computers, Environment and Urban Systems, 21*(3), 259–276.

Ma, Y., Zhao, Y., Liu, J., He, X., Wang, B., & Fu, S. (2020). Effects of Temperature Variation and Humidity on the Mortality of COVID-19 in Wuhan. *medRxiv*.
Mishra, S. V. (2018). Urban deprivation in a global south city-a neighborhood scale study of Kolkata, India. *Habitat International, 80*, 1–10. https://doi.org/10.1016/j.habitatint.2018.08.006
Mollalo, A., Mao, L., Rashidi, P., & Glass, G. E. (2019). A GIS-based artificial neural network model for spatial distribution of tuberculosis across the continental United States. *International Journal of Environmental Research and Public Health, 16*(1), 157.
Mukherjee, S., Yang, X., Shan, W., Samarakoon, W., Karakalos, S., Cullen, D. A., … Wu, G. (2020). Atomically Dispersed Single Ni Site Catalysts for Nitrogen Reduction toward Electrochemical Ammonia Synthesis Using N2 and H2O. *Small Methods*.
Musse, M. A., Barona, D. A., & Rodriguez, L. M. S. (2018). Urban environmental quality assessment using remote sensing and census data. *International Journal of Applied Earth Observation and Geoinformation, 71*, 95–108.
Naddeo, V., & Liu, H. (2020). Editorial Perspectives: 2019 novel coronavirus (SARS-CoV-2): what is its fate in urban water cycle and how can the water research community respond? *Environmental Science: Water Research & Technology, 6*(5), 1213–1216.
Nichol, J., & Wong, M. S. (2009). Mapping urban environmental quality using satellite data and multiple parameters. *Environment and Planning B Planning and Design, 36*(1), 170–185. https://doi.org/10.1068/b34034
Niu, T., Chen, Y., & Yuan, Y. (2020). Measuring urban poverty using multi-source data and a random forest algorithm: A case study in Guangzhou. *Sustainable Cities and Society, 54*, Article 102014. https://doi.org/10.1016/j.scs.2020.102014
Núñez-Delgado, A. (2020). What do we knowabout the SARS-CoV-2 coronavirus in the environment? *Science of the Total Environment*. https://doi.org/10.1016/j.scitotenv.2020.138647. Elsevier.
Ogneva-Himmelberger, Y., Rakshit, R., & Pearsall, H. (2012). Examining the impact of environmental factors on quality of life across Massachusetts. *The Professional Geographer, 65*(2), 187–204. https://doi.org/10.1080/00330124.2011.639631
Patel, J. A., Nielsen, F. B. H., Badiani, A. A., Assi, S., Unadkat, V. A., Patel, B., … Wardle, H. (2020). Poverty, inequality and COVID-19: the forgotten vulnerable. *Public Health, 183*, 110.
Phukan, D. K. (2014). Levels of some basic amenities in the slums and their impacts on ecology: a case study of Jorhat City, Assam. *International Journal of Science and Research, 3*(1), 71–74.
Pinheiro, J. C., & Bates, D. M. (2000). *Mixed Effects Models in S and S-plus*. New York: Springer, 528pp.
Portela, C. I., Massi, K. G., Rodrigues, T., & Alcântara, E. (2020). Impact of urban and industrial features on land surface temperature: Evidences from satellite thermal indices. *Sustainable Cities and Society, 56*, Article 102100. https://doi.org/10.1016/j.scs.2020.102100
Rahman, A., Kumar, Y., Fazal, S., & Bhaskaran, S. (2011). Urbanization and quality of urban environment using remote sensing and GIS techniques in East Delhi-India. *Journal of Geographic Information System, 3*, 62–84. https://doi.org/10.4236/jgis.2011.31005
Rao, K. R. M., Kant, Y., Gahlaut, N., & Roy, P. S. (2012). Assessment of quality of life in Uttarakhand, India using geospatial techniques. *Geocarto International, 27*(4), 315–328.
Rashed, E. A., Kodera, S., Gomez-Tames, J., & Hirata, A. (2020). Influence of absolute humidity, temperature and population density on COVID-19 spread and decay durations: Multi-prefecture study in Japan. *International Journal of Environmental Research and Public Health, 17*(15), 5354.
Rocklöv, J., & Sjödin, H. (2020). High population densities catalyse the spread of COVID-19. *Journal of Travel Medicine, 27*(3). taaa038.
Sajjad, H. (2014). Living standards and health problems of lesser fortunate slum dwellers: evidence from an Indian City. *International Journal of Environmental Protection and Policy, 2*, 54.
Sannigrahi, S., Pilla, F., Basu, B., Basu, A. S., & Molter, A. (2020). Examining the association between socio-demographic composition and COVID-19 fatalities in the European region using spatial regression approach. *Sustainable Cities and Society, 62*, Article 102418. https://doi.org/10.1016/j.scs.2020.102418
Santana, L. M., Escobar Jaramillo, L. A., & Capote, P. A. (2010). Estimación de un índice de calidad ambiental urbano, a partir de imágenes. *Revista de Geografía Norte Grande, 45*, 77–95.
Saroj, S. K., Goli, S., Rana, M. J., & Choudhary, B. K. (2020). Availability, accessibility, and inequalities of water, sanitation, and hygiene (WASH) services in Indian metro cities. *Sustainable Cities and Society, 54*, Article 101878. https://doi.org/10.1016/j.scs.2019.101878
Sejati, A. W., Buchori, I., & Rudiarto, I. (2019). The spatio-temporal trends of urban growth and surface urban heat islands over two decades in the Semarang Metropolitan Region. *Sustainable Cities and Society, 46*, Article 101432. https://doi.org/10.1016/j.scs.2019.101432
Shahbaz, M., Sbia, R., Hamdi, H., & Ozturk, I. (2014). Economic growth, electricity consumption, urbanization and environmental degradation relationship in United Arab Emirates. *Ecological Indicators, 45*, 622–631.
Silva, L. T., & Mendes, J. F. G. (2012). City noise-air: an environmental quality index for cities. *Sustainable Cities Society, 4*, 1–11.
Stathopoulou, M., Iacovides, S., & Cartalis, C. (2012). Quality of life in metropolitan Athens, using satellite and census data: comparison between 1991 and 2001. *The Journal of Heat Island Institute International, 7*, 25–32.
Stossel, Z., Kissinger, M., & Meir, A. (2015). Assessing the state of environmental quality in cities e a multi- component urban performance (EMCUP) index. *Environment Pollution, 206*, 679–687.
Sultana, S., & Satyanarayana, A. N. V. (2020). Assessment of urbanisation and urban heat island intensities using landsat imageries during 2000–2018 over a sub-tropical Indian City. *Sustainable Cities and Society, 52*, Article 101846. https://doi.org/10.1016/j.scs.2019.101846
Sun, J., He, W. T., Wang, L., Lai, A., Ji, X., Zhai, X., & Veit, M. (2020). COVID-19: epidemiology, evolution, and cross-disciplinary perspectives. *Trends in Molecular Medicine*. https://doi.org/10.1016/j.molmed.2020.02.008
Sussman, H. S., Raghavendra, A., & Zhou, L. (2019). Impacts of increased urbanization on surface temperature, vegetation, and aerosols over Bengaluru, India. *Remote Sensing Applications: Society and Environment, 16*, 100261.
Taghizadeh-Hesary, F., & Akbari, H. (2020). *The powerful immune system against powerful COVID-19: a hypothesis. Preprints 2020*, 2020040101. https://doi.org/10.20944/preprints202004.0101.v1.
Tomar, A., & Gupta, N. (2020). Prediction for the spread of COVID-19 in India and effectiveness of preventive measures. *Science of The Total Environment, 728*, Article 138762. https://doi.org/10.1016/j.scitotenv.2020.138762
United Nations. (2020). *The Social Impact of COVID-19*. Retrieved from https://www.un.org/development/desa/dspd/2020/04/social-impact-of-covid-19/.
United States Geological Survey (USGS) website (https://earthexplorer.usgs.gov).
Wang, Q., & Su, M. (2020). A preliminary assessment of the impact of COVID-19 on environment–A case study of China. *Science of the Total Environment*, 138915. https://doi.org/10.1016/j.scitotenv.2020.138915
Wang, Q., & Wang, S. (2020). Preventing carbon emission retaliatory rebound post-COVID-19 requires expanding free trade and improving energy efficiency. *Science of The Total Environment, 746*, Article 141158. https://doi.org/10.1016/j.scitotenv.2020.141158
Wang, L., Li, J., Guo, S., Xie, N., Yao, L., Cao, Y., et al. (2020). Real-time estimation and prediction of mortality caused by COVID-19 with patient information-based algorithm. *Science of The Total Environment*, 138394.
World Health Organization (WHO). (2020a). *Rolling Updates on Coronavirus Disease (COVID-19)*. Retrieved from https://www.who.int/emergencies/diseases/novel-coronavirus-2019/events-as-they-happen.
World Health Organization (WHO). (2020b). *Report of the WHO-China Joint Mission on Coronavirus Disease 2019 (COVID-19)*. Retrieved from https://www.who.int/docs/default-source/coronaviruse/who-china-joint-mission-on-covid-19-final-report.pdf.
World Health Organization (WHO). (2020c). *Coronavirus Disease 2019 (COVID-19) Situation Report-103*. Retrieved from https://www.who.int/docs/default-source/coronaviruse/situation-reports/20200502-covid-19-sitrep103.pdf?sfvrsn=d95e76d8_4.
Wu, X., Nethery, R. C., Sabath, B. M., Braun, D., & Dominici, F. (2020). *Exposure to Air Pollution and COVID-19 Mortality in the United States*. https://doi.org/10.1101/2020.04.05.20054502
Yang, J., Sun, J., Ge, Q., & Li, X. (2017). Assessing the impacts of urbanization-associated green space on urban land surface temperature: A case study of Dalian, China. *Urban Forestry & Urban Greening, 22*, 1–10.
Yao, R., Cao, J., Wang, L., Zhang, W., & Wu, X. (2019). Urbanization effects on vegetation cover in major African cities during 2001-2017. *International Journal of Applied Earth Observation and Geoinformation, 75*, 44–53.
Yongjiana, Z., Jingubc, X., Fengmingb, H., & Liqingb, C. (2020). Association between shortterm exposure to air pollution and COVID-19 infection: evidence from China. *Science of the Total Environment*. https://doi.org/10.1016/j.scitotenv.2020.138704. Elsevier.
Zeileis, A., Kleiber, C., & Jackman, S. (2008). Regression models for count data in R. *Journal of Statistical Software, 27*, 1–25.
Zeng, W. S. (2015). Using nonlinear mixed model and dummy variable model approaches to construct origin-based single tree biomass equations. *Trees (Berlin), 29*, Article 275e283.
Zhang, Y., & Sun, L. (2019). Spatial-temporal impacts of urban land use land cover on land surface temperature: Case studies of two Canadian urban areas. *International Journal of Applied Earth Observation and Geoinformation, 75*, 171–181.
Zhang, X., Estoque, R. C., & Murayama, Y. (2017). An urban heat island study in Nanchang City, China based on land surface temperature and social-ecological variables. *Sustainable cities and society, 32*, 557–568. https://doi.org/10.1016/j.scs.2017.05.005
Zhu, Y., & Xie, J. (2020). Association between ambient temperature and COVID-19 infection in122 cities from China. *Science of the Total Environment*. https://doi.org/10.1016/j.scitotenv.2020.138704. Elsevier.